Quantification of Cyclic Electron Flow in Spinach Leaf Discs

Jiancun Kou[a,b], Shunichi Takahashi[b], Riichi Oguchi[b], Murray R Badger[b], Wah Soon Chow[b,*]

[a] North-West Agricultural & Forestry University, Yangling, Shaanxi 712100, China;
[b] Division of Plant Science, Research School of Biology, College of Medicine, Biology and Environment, The Australian National University, Canberra, ACT 0200, Australia.
[*]Corresponding author. Tel. No. +61 2 6125 3980; Fax No. +61 2 6125 8056; E-mail: Fred.Chow@anu.edu.au.

Abstract: We quantified the photosynthetic cyclic electron flux (CEF) around Photosystem I as the difference between the total electron flux through PS I (ETR1) and the linear electron flux through both photosystems. Both measurements were made in the whole tissue of spinach leaf discs illuminated in the same geometry and in CO_2-enriched air to suppress photorespiration. (1) CEF was negligibly small below 300 μmol photons m^{-2} s^{-1}. Above this irradiance, CEF increased approximately linearly up to the highest irradiance used (1,900 μmol photons $m^{-2}s^{-1}$). (2) CEF at a fixed irradiance of 980 μmol m^{-2} s^{-1} increased by a factor of almost 3 as the temperature was increased from 5 °C to 40 °C. It did not decline, even when the linear electron flux decreased at high temperatures. (3) Antimycin A, at a high concentration, decreased CEF to about 10% of the control value without affecting the linear electron flux. This method appears to be reliable for quantifying CEF non-intrusively. By contrast, estimation of the linear electron flux from chlorophyll fluorescence over-estimated CEF in the above treatments.

Keywords: Antimycin A; Cyclic electron flow; Linear electron flow; P700; Photosystem I

Introduction

The significance, mechanisms and roles of the photosynthetic cyclic electron flux (CEF) have been intensely studied (for reviews, see Bendall and Manasse, 1995; Allen, 2003; Johnson, 2005; Joliot and Joliot, 2006). Unfortunately, efforts to elucidate the importance of CEF have been hampered by the difficulty of quantifying CEF due to the absence of a net product of cyclic electron flow.

In this study we sought to quantify CEF by devising a method that is simple to apply routinely, that uses white light to simulate sunlight and that is relatively non-intrusive. Our approach was to measure the total electron flux (ETR1) through Photosystem I (PSI) and the linear electron flux (LINEAR) through PSII and PSI in series. Crucially, we ensured that both ETR 1 and LINEAR were measured in the whole tissue of a leaf disc illuminated in the same geometry in 1% CO_2. CEF was then calculated as CEF = ETR1 – LINEAR.

Materials and Methods

Spinacea oleracea L. (cv. Yates hybrid 102) plants were grown in a glasshouse at approximately 30/15 ºC (day/night) under natural light in autumn and winter. The plants were provided with a nutrient solution, supplemented by a slow release fertilizer.

When required, leaf discs (1.5 cm^2) were immersed in water, or a selected concentration of antimycin A, vacuum infiltrated using a water-driven pump for about 30 s, blotted with absorbent paper, and allowed to evaporate off the excess intercellular water in darkness for ~ 30 min before measurement.

LINEAR was determined by measurement of O_2 evolution by a leaf disc placed in a gas-phase Hansatech O_2 electrode equipped with an adaptor that accepts a multifurcated light guide. The electrode chamber contained 1% CO_2. White projector light filtered by a Calflex C heat-reflecting filter and neutral-density filter(s) was passed through one branch of the light guide. O_2 evolution was measured

T. Kuang et al., *Photosynthesis Research for Food, Fuel and the Future*

over several minutes until a steady rate was reached. The post-illumination drift was added algebraically to the oxygen evolution rate during illumination, and the sum was multiplied by four to obtain LINEAR.

ETR1 was determined by redox changes of P700, the special chlorophyll (Chl) pair in PSI, with an ED-P700DW unit attached to a PAM fluorometer (Walz, Germany) (time constant = 95 μs). Prior to P700 measurements, a leaf disc had been brought to a steady photosynthetic state by illumination with white actinic light of a selected irradiance (I) for > 10 min during which O_2 evolution and light-acclimated Chl fluorescence yields were obtained. To ensure retention of the steady state after the earlier measurements, each leaf disc was immediately re-illuminated with the same actinic light for 9 s, defined by a shutter controlled by a pulse generator (Model 565, Berkeley Nucleonics Corporation, U.S.A.).

During each 9-s interval, at time = 8.80 s (corresponding to the time point −50 ms in Fig. 1A), data acquisition was started by a trigger from a second terminal of the pulse generator. At 8.85 s, a strong far-red light (FR, ~ 2,000 μmol photons m^{-2} s^{-1}) from a light-emitting diode array (emission peak 741 nm, LED735-66-60, Roithner LaserTechnik, Austria) was triggered on for 100 ms using a trigger from a third terminal of the pulse generator. The strong FR light further oxidized a fraction of the P700 even in the presence of white actinic light, depleting electrons from the inter-system chain, so that the subsequent saturating pulse (see immediately below) oxidizes P700 maximally in the light-acclimated state (Siebke *et al*., 1997). While the strong FR light was still on, at time = 8.90 s, a saturating light pulse (~9,000 μmol photons m^{-2} s^{-1}) was turned on by an electronic shutter for 10 ms, triggered by a fourth terminal of the pulse generator. Finally, the actinic light was turned off at 9.0 s. Data acquisition continued for a further 85 ms to obtain the baseline corresponding to zero $P700^+$. On completion of data acquisition, another 9-s sequence of illumination operations was started, thereby maintaining steady-state photosynthesis. Nine traces were averaged by software (written by the late A. B. Hope) to improve signal:noise.

Next, we determined the maximum extent of P700 oxidation under conditions with no limitation on the acceptor side of PS I. First, we established a steady state by illumination with weak far-red light (~12 μmol photons m^{-2} s^{-1} at 723 nm, from an LED) for > 10 s (Fig. 1B). Then we superimposed a saturating single-turnover flash on the weak far-red light. Flashes were given at 0.2 Hz, and 9 consecutive signals were averaged. The maximum signal immediately after the flash, $[P700^+]_{max}$, was taken as the total photo-oxidizable P700. The photochemical yield of PS I is given by $Y(I) = b/[P700^+]_{max}$, where b is the signal interval b in Fig. 1A (Klughammer and Schreiber, 2007). ETR1 was calculated as $Y(I) \times I \times 0.85 \times 0.5$ for the white actinic light used.

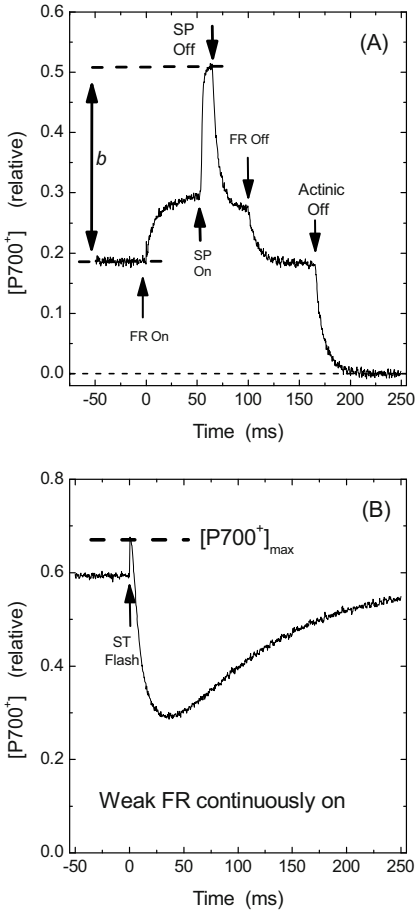

Fig. 1 Measurement of the photochemical yield of PS I in two steps. (A) When steady-state photosynthesis was occurring at 980 μmol m^{-2} s^{-1} with a steady $[P700^+]$, strong far-red light (FR) was turned on at t = 0 for 100 ms to further photo-oxidize P700. At t = 50 ms, a 10-ms saturating light pulse (SP) photo-oxidized P700 fully. Actinic illumination ended at t = 166 ms. The signal interval b represents the P700 still available for photo-oxidation. (B) Maximum photo-oxidizable P700 was obtained by illuminating a leaf disc with weak continuous far-red light to attain ~88% oxidation in the steady state. Then a single-turnover saturating flash photo-oxidized the remaining P700. The peak immediately after the flash is $[P700^+]_{max}$, the ratio $b/[P700^+]_{max}$ being the photochemical yield of PS I as defined by Klughammer and Schreiber (2007).

We also measured the quantum yield of PSII photochemistry averaged over open and closed traps

(Genty *et al*., 1989), *viz.* $\phi_{PS\ II} = (1 - F_s'/F_m')$, where F_s' is the fluorescence yield at steady state and F_m' the maximum fluorescence yield in the light-acclimated state. ETR2, the electron flux through PSII, was calculated as $(1 - F_s'/F_m') \times I \times 0.85 \times 0.5$, for comparison with LINEAR.

Results and Discussion

Electron Fluxes in Response to Irradiance

ETR1, the total electron flux through PS I, increased with irradiance, showing no saturation even at the highest irradiance (Fig. 2). By contrast, LINEAR peaked at about 1500 µmol e^- m^{-2} s^{-1}. The maximum LINEAR was ~188 µmol electrons m^{-2} s^{-1} (≡ 47 µmol O_2 m^{-2} s^{-1}). CEF = ERT1 – LINEAR was very small below 300 µmol m^{-2} s^{-1}, above which it increased approximately linearly with irradiance (Fig. 2). At the highest *I*, CEF almost equalled the linear rate. ETR2, assayed by Chl *a* fluorescence, underestimated the whole-tissue linear rate measured by O_2 evolution, the discrepancy increasing with irradiance.

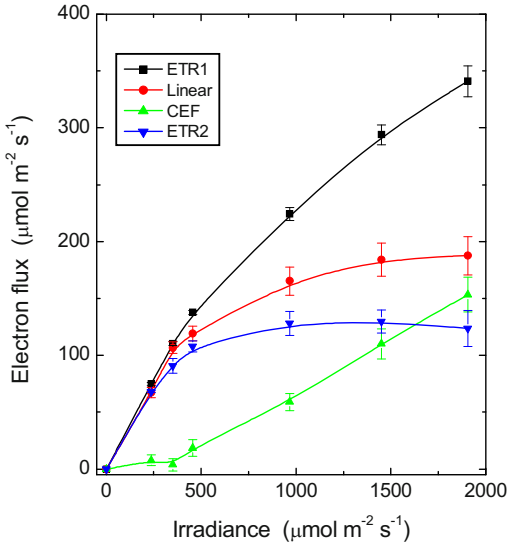

Fig. 2 Response of steady-state electron fluxes to irradiance. ETR1 is the total electron flux through PS I, and LINEAR the linear electron flux through both photosystems, both being whole-tissue measurements. CEF = ETR1 – LINEAR. ETR2 is the electron flux through PS II based on Chl fluorescence measurements. Values are means ± SE (n = 14 leaf discs).

The negligibly small CEF at $I < 300$ µmol m^{-2} s^{-1} (Fig. 2) is expected since the Calvin-Benson cycle was able to use the majority of NADPH at low irradiance, leaving little spare reduced ferredoxin for cyclic electron flow. When the linear electron flow reached a saturated rate at high irradiance, however, reduced ferredoxin accumulated, and CEF approached the linear electron flux.

Electron Fluxes in Response to Temperature

At a fixed irradiance of 980 µmol m^{-2} s^{-1}, ETR1 increased steadily with temperature until it peaked at about 32 °C, and then decreased above this temperature (Fig. 3). LINEAR, assayed by O_2 evolution, followed a similar pattern, but it peaked at a temperature slightly below 30 °C. The difference, representing CEF, increased steadily with temperature.

It has been suggested that cyclic electron flow is activated by high temperature (Bukhov *et al*., 1999; Clarke and Johnson, 2001). In our study, cyclic electron flow increased by a factor of almost 3 when the temperature was raised from 5 °C to 40 °C (Fig. 2). Liner declined between 32.5 °C and 40 °C, perhaps because of down-stream limitation in carbon assimilation. By contrast, CEF did not decrease at 40 °C (Fig. 3). If carbon assimilation decreased at high temperatures, reduced ferredoxin would accumulate, favouring cyclic electron flow, particularly if the warm temperature facilitated the diffusion of ferredoxin or accelerated enzymatic reactions involved in cyclic electron flow.

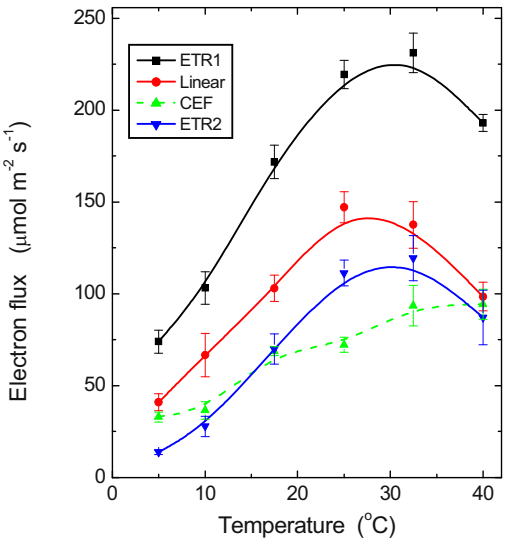

Fig. 3 Variation of steady-state electron fluxes with temperature. A fixed irradiance of 980 µmol m^{-2} s^{-1} was used. Values are means ± SE (n = 14 leaf discs).

Inhibition of CEF by Antimycin A

Antimycin A inhibits the ferredoxin-dependent cyclic electron flux. In Fig. 4A, ETR1 decreased

towards an asymptotic value. However, the inhibitor had no effect on the linear flux assayed by O_2 evolution. The difference between the two fluxes indicates that CEF decreased steadily with increase in [antimycin A], reaching a value of about 10% of that of control leaf tissue. With the loss of CEF, the fraction of excitation energy dissipated non-photochemically in a light-regulated manner (ϕ_{NPQ}) decreased by about 34% (Fig. 4B), *despite* the constancy of linear electron flow. That is, CEF contributed to ϕ_{NPQ} by producing a ΔpH.

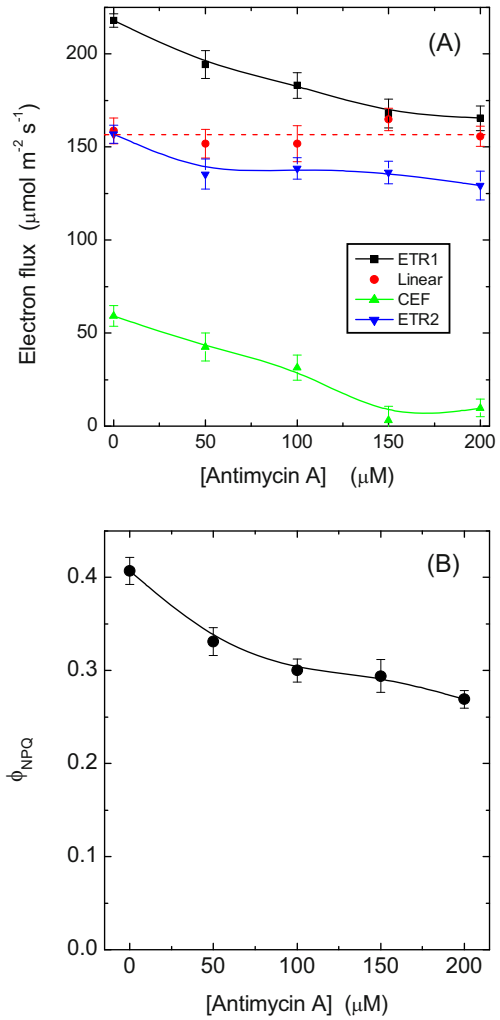

Fig. 4 (A) Variation of steady-state electron fluxes with [antimycin A] used to infiltrate leaf discs, at a fixed irradiance of 980 μmol m^{-2} s^{-1}. Values are means ± SE (n = 15 leaf discs). (B) ϕ_{NPQ}, the fraction of light absorbed by the PS II antennae that is dissipated as heat via ΔpH- and xanthophylls-regulated processes is plotted against [antimycin A].

Our observation that antimycin A largely abolished CEF suggests that (1) a cyclic path involving the NAD(P)H dehydrogenase may be a minor pathway, and (2) charge recombination in PSI (which would not contribute to ϕ_{NPQ}) might have only a small role in determining Y(I) under the experimental conditions.

Acknowledgements

A China Scholarship Council fellowship (to JK) and grants from the Australian Research Council to WSC (DP1093827) and MRB (Centre of Excellence in Plant Energy Biology) supported this work.

References

Allen JF (2003) Cyclic, Pseudocyclic and Noncyclic Photophosphorylation: New Links in the Chain. Trends Plant Sci 8: 15-19

Bendall DS, Manasse R (1995) Cyclic Photophosphorylation and Electron Transport. Biochim Biophys Acta 1229: 23-38

Bukhov NG, Wiese C, Neimanis S, Heber U (1999) Heat Sensitivity of Chloroplasts and Leaves: Leakage of Protons from Thylakoids and Reversible Activation of Cyclic Electron Transport. Photosynth Res 59: 81-93

Clarke JE, Johnson GN (2001) In Vivo Temperature Dependence of Cyclic and Pseudocyclic Electron Transport inBarley. Planta 212: 808-816

Genty B, Briantais JM, Baker NR (1989) The Relationship between the Quantum Yield of Photosynthetic Electron Transport and Quenching of Chlorophyll Fluorescence. Biochim Biophys Acta 990: 87-92

Johnson GN (2005) Cyclic Electron Transport in C_3 Plants: Fact or Artefact? J Exp Bot 56: 407-416

Joliot P, Joliot A (2006) Cyclic Electron Flow in C3 Plants. Biochim Biophys Acta 1757: 362-368

Klughammer C, Schreiber U (2007) Saturation Pulse Method for Assessment of Energy Conversion in PSI http://www.walz.com/e_journal/pdfs/PAN07002.pdf

Siebke K, Caemmerer S von, Badger M, Furbank RT (1997) Expressing an RbcS Antisense Gene in Transgenic Flaveria Bidentis Leads to an Increased Quantum Requirement for CO_2 Fixed in Photosystems I and II. Plant Physiol 115: 1163-1174